

THE ROLE OF CD90 IN BREAST CANCER TUMOR PROGRESSION

by

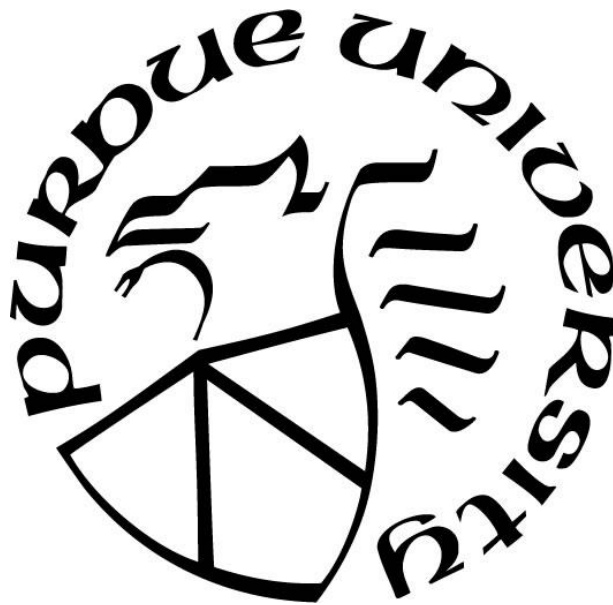
Monica Kasturi Chanda

A Thesis

Submitted to the Faculty of Purdue University

In Partial Fulfillment of the Requirements for the degree of

Master of Science in Biomedical Engineering



Weldon School of Biomedical Engineering

West Lafayette, Indiana

August 2020

**THE PURDUE UNIVERSITY GRADUATE SCHOOL
STATEMENT OF COMMITTEE APPROVAL**

Dr. Luis Solorio, Chair

Weldon School of Biomedical Engineering

Dr. Michael Wendt

Department of Medicinal Chemistry and Molecular Pharmacology

Dr. Sherry Harbin

Weldon School of Biomedical Engineering

Approved by:

Dr. George R. Wodicka

Dedicated to my loving and supportive family

ACKNOWLEDGMENTS

This work was supported by the National Cancer Institute (R0CA19829 to L.S.), as well as the by the NIH Shared Instrumentation Grant S10DO20029. I would like to thank Dr. Luis Solorio for his support throughout my time at Purdue. I would also like to thank the Solorio Lab, especially Brian Jun, Sarah Libring, and Kevin Buno for their guidance and help. Lastly, I would like to thank Juan Sebastian Paez for his help with creating the knockdowns for this project.

TABLE OF CONTENTS

LIST OF FIGURES	6
ABSTRACT.....	8
1. INTRODUCTION	9
2. METHODS	13
2.1 Culturing Methods	13
2.2 Generation of Ca1h CD90 Knockdown Cell Line	13
2.3 Flow Cytometry	13
2.4 Immunofluorescence.....	14
2.5 Evaluation of Fibronectin Production.....	14
2.6 Fibronectin Coated Scaffold System	15
2.7 Cell Proliferation 3D Coculture Assay	15
2.8 Statistical Analysis.....	15
3. RESULTS	17
3.1 Expression of MSC markers in epithelial and mesenchymal-like cells.....	17
3.2 Characterization of CD90 Knockdowns	21
3.3 Fibronectin Expression	24
3.4 Early Metastatic Niche Model	25
3.5 Effect of Coculture on Cell Proliferation.....	27
4. DISCUSSION.....	29
REFERENCES	31

LIST OF FIGURES

- Figure 1. Visual representation of epithelial to mesenchymal transition.** Cells lose their apical-basal polarity and tight cell junctions and begin to spread out with anterior-posterior polarity. . 10
- Figure 2. An alteration in MSC markers decreases patient survival.** Analysis of the METABRIC dataset for overall survival in months for patients with alterations to the genes for CD90 (THY1), CD105 (ENG), and CD73 (NT5E). Patients with an alteration in more than one of the genes are not displayed. Analysis was done using cBioPortal [25]–[27]. 11
- Figure 3. Positive and negative controls for MSC marker analysis. A.)** ASCs as a positive control and their isotype stained for CD90, CD105, and CD73. **B.)** K562s as a negative control and their isotype stained for CD90, CD105, and CD73. 18
- Figure 4. Mesenchymal-like cells express MSC markers, while epithelial-like cells do not. A.)** Flow cytometry graphs showing gating of markers. **B.)** Percent expression of markers in ASC, Ca1h, Ca1a, Ca1hFN30 (n=3). An ANOVA followed by a Tukey test was performed for statistical analysis. Asterisk denotes statistically significant differences in the populations ($p < 0.05$)...... 19
- Figure 5. Immunofluorescence images of MSC markers confirm flow cytometry analysis.** CD90 in red, CD105 in yellow, CD73 in magenta on ASC, Ca1h, Ca1a, and Ca1hFN30. All scale bars indicate 50 μ m. 20
- Figure 6. Characterization of CD90 knockdowns using flow cytometry. A.)** Flow cytometry graphs showing gating of CD90. **B.)** Percent expression of CD90 in wild type Ca1h, and knockdowns TH02 and TH03 (n=3). **C.)** Flow cytometry graphs showing gating of CD24 and CD44. **D.)** Percent expression of CD44⁺/CD24⁻ in wild type Ca1h, and knockdowns TH02 and TH03 (n=3). An ANOVA followed by a Tukey test was performed for statistical analysis. Asterisk denotes statistically significant differences in the populations ($p < 0.05$). 22
- Figure 7. CD90 knockdown shows transition to epithelial-like phenotype.** Phase contrast images of scram Ca1h and CD90 knockdowns. 23
- Figure 8. CD90 knockdowns shows expression of E-cadherin.** 23
- Figure 9. CD90 knockdowns still express fibronectin. A.)** Human fibronectin ELISA results in ug/ml. **B.)** Immunofluorescence staining for fibronectin. Fluorescence intensity analysis was done using ImageJ. Scale bar indicates 100 μ m. 25
- Figure 10. CD44⁺/CD24⁻ populations increased after culturing on fibronectin coated scaffolds. A.)** Flow cytometry graphs showing gating of CD44⁺/CD24⁻ population. **B.)** Percent of population that is CD44⁺/CD24⁻ on scaffolds in comparison to 2D (n=1). 26
- Figure 11. CD90⁺ population does not shift after culturing on fibronectin coated scaffolds.** Flow cytometry analysis for Ca1h, TH03, and Ca1a cultured on scaffolds (n=1). 27
- Figure 12. Coculture analysis shows increase proliferation and migration of Ca1a when cocultured with ASCs compared to TH03. A.)** Normalized proliferation of Ca1a cells alone and in coculture over 3.25 days. **B.)** Final normalized cell count on day 3.25 of coculture. **C.)** Distanced

traveled by Ca1a cells in μm . An ANOVA followed by a Tukey test was performed for statistical analysis. Asterisk denotes statistically significant differences in the populations ($p < 0.05$)..... 28

ABSTRACT

Breast cancer is the most common cancer among women, with effective treatments if the disease stays local. However, if the tumor metastasizes, patient outcomes are significantly reduced. Mesenchymal stem cells (MSC) have been shown to enhance metastasis by facilitating invasion and tumor outgrowth. MCF10A Ca1h cells, a mesenchymal-like cell line, have been shown to promote metastasis in a murine model and enhance the survival and proliferation of their epithelial counterpart (Ca1a) in coculture. We have established the presence of the classic MSC markers, CD90, CD105, and CD73, on the Ca1h cells and observe a decrease in the CD90⁺ population in the Ca1a and fibronectin knockdown Ca1h cells. To examine the effects of this decreased expression, a CD90 knockdown of Ca1h cells was created using lenti-viral transduction. A decrease in fibronectin levels was seen in the CD90 knockdowns, along with a change in morphological characteristics of the cells. To investigate the influence of a 3D microenvironment on cell phenotype, they were also cultured on fibronectin coated scaffolds and evaluated for CD44/CD24 expression. Lastly, the knockdowns were cocultured with the Ca1a cells in a 3D hydrogel to assess the impact of coculture on survival and proliferation. We found that the CD90 knockdowns take on epithelial-like characteristics and decrease survival of Ca1a cells in coculture. These findings suggest that CD90 is necessary to maintain a mesenchymal phenotype and could be used as a target for therapies to prevent metastasis.

1. INTRODUCTION

Breast cancer is the most common cancer among women, accounting for 30% of female cancers [1]. If caught early, most patients will survive. However, as the disease progresses survival decreases, with about 90% of cancer associated deaths being caused by metastasis [2]. Metastasis is the multistage process by which disseminated cancer cells form secondary tumors [3], [4]. The metastatic process is aided by tumor heterogeneity which results in varying cell types that differ in proliferative and invasive properties [5]. As a consequence of the cellular heterogeneity, unique paracrine signaling dynamics can develop within the tumor microenvironment and dictate cell fate [6]. One potential source of heterogeneity within the tumor microenvironment is a differential response to cell-cell and cell-environment stimuli that can induce varying degrees of an epithelial to mesenchymal transition (EMT) within the population of tumor cells [7].

During EMT, epithelial cells lose their cell-to-cell connections and apical-basal polarity to assume a more spread out phenotype and acquire more mesenchymal-like characteristics with greater migratory ability (Figure 1) [5], [8], [9]. An epithelial state can be identified using the marker E-cadherin, whose expression is lost as the cell becomes more mesenchymal-like, gaining expression of markers like fibronectin [10]. This process of EMT results in tumor cells that range across a spectrum of epithelial to mesenchymal phenotypes promoting tumor growth and metastasis [7], [10]. A recent study suggests that some cells that have lost their epithelial characteristics and have increased expression of genes relating to the mesenchymal phenotype, have reduced ability to form tumors [11]. Stably mesenchymal tumor cells proliferate slowly allowing them to readily invade tissues, but do not have the capacity to form secondary tumors and complete the metastatic cascade. Instead, they contribute to metastatic progression by taking a more supportive role in the tumor microenvironment [12]. A recent study utilizing *in vitro* 3D collagen cultures found that alone, epithelial tumor cells could not survive for more than four days. However, when in a co-culture with the fibronectin producing mesenchymal tumor cells the epithelial population had greater survival, constant proliferation, and could migrate farther with greater velocity [13]. These studies suggest that cells that have undergone EMT may facilitate survival and are necessary to prepare the tumor microenvironment for tumor outgrowth.

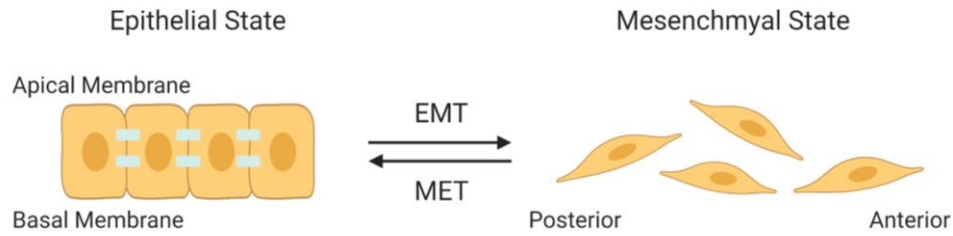


Figure 1. Visual representation of epithelial to mesenchymal transition. Cells lose their apical-basal polarity and tight cell junctions and begin to spread out with anterior-posterior polarity.

EMT is not only associated with cancer progression but is also seen as a normal program for wound repair. Keratinocytes, the epithelial cells that reside in the skin, transition to a dedifferentiated, more mesenchymal-like state. In this state, these cells gain the ability to migrate across the wound and facilitate the formation of a new epithelial layer [14]. Mesenchymal stem cells (MSC) also play an important role throughout the wound healing process, from regulating inflammation to promoting tissue growth and remodeling [14]–[16]. These properties are translated to cancer, as it is believed that mesenchymal stem cells migrate to tumors as they would during wound healing [17]. In breast cancer, it has been hypothesized that mesenchymal stem cells are involved in development of the tumor niche, and have also been shown to promote metastasis [18]–[20]. Their immunosuppressive abilities support and stabilize the tumor microenvironment, and through paracrine signaling, MSCs can facilitate tumor growth and invasion [21], [22]. A defining aspect of MSCs is their expression of CD90, CD105, and CD73 [23], [24].

These markers seem to play a role in survival of breast cancer patients. Using cBioPortal, the Molecular Taxonomy of Breast Cancer International Consortium (METABRIC) database, patient survival for those with an alteration, whether it be a mutation, amplification, or deletion in the genes for CD90 (THY1), CD73 (NT5E), and CD105 (ENG), was evaluated [25]–[27]. Overall survival between each gene was compared (Figure 2). This data shows that CD105 (ENG), a marker for angiogenesis and neovascularization, has the lowest mean survival, but it has already been identified as a marker for metastasis in breast cancer [28], [29]. CD73 (NT5E), shows the highest mean survival, and seems to play a role in immune suppression in the tumor microenvironment [30]. The role of CD90 is less understood, but it does play a role in matrix adhesion, and can communicate with the local microenvironment through its integrin and heparin

binding domains [31]. Recent studies have indicated that the CD90 positive population increases in response to fibronectin rich environments in AT-3 mouse mammary carcinoma cells [33]. Furthermore, it has been shown that MSCs cultured with MDA-MB-231 cells significantly increased proliferation of the MDA-MB-231 population and induce expression of CD90 [34].

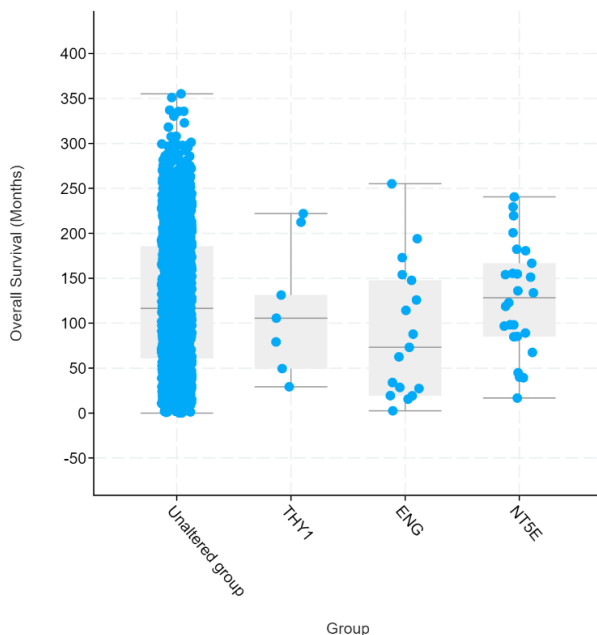


Figure 2. An alteration in MSC markers decreases patient survival. Analysis of the METABRIC dataset for overall survival in months for patients with alterations to the genes for CD90 (THY1), CD105 (ENG), and CD73 (NT5E). Patients with an alteration in more than one of the genes are not displayed. Analysis was done using cBioPortal [25]–[27].

CD90 is a membrane bound, lipid anchored protein that is encoded for by the gene THY1. It is involved in cell-cell and cell-matrix interactions. In humans, CD90 can be found in neurons, T cells, endothelial cells, mesenchymal stem cells, hematopoietic stem cells, and fibroblasts [31], [32]. In fibroblasts, THY1 is known to regulate focal adhesions, cytoskeleton arrangement, and migratory ability through Src-mediated Rho GTPase activation [35]. CD90 also plays a role in cancer, though this varies with cancer type. In some cancers, it may act as a tumor suppressor, while in other it can assist with tumor growth and sometimes promote invasion and metastasis [32]. In breast cancer, CD90 expression has been correlated to worse prognosis [36]. CD90 positive cells have been identified in the invasive front of tumors and possess a migratory ability that may be attributed to epithelial to mesenchymal transition [37], [38]. It is believed that CD90 positive

cells lay on the outside of the tumor, and give rise to cells that lack CD90 which migrate toward the center of the tumor and proliferate [37].

We investigated the role of CD90 in breast cancer using the MCF10-Ca1a (Ca1a) epithelial-like cells and the MCF10-Ca1h (Ca1h) mesenchymal-like cells. We also utilized Ca1hFN30 fibronectin knockdown Ca1h cells, which have an epithelial-like phenotype. We hypothesize that the Ca1h cells will be positive for CD90, CD73, and CD105, and that by knocking down CD90, these cells will lose their mesenchymal-like characteristics. Previous studies have shown that these Ca1h cells promote metastasis in a murine model and promote survival and proliferation in coculture as seen in studies with the MSCs [12], [13], [34]. These cells also do not directly participate in new tumor development, and instead seem to take a more supportive role in the tumor microenvironment, much like MSCs [21]. By knocking down CD90 in these cells, we believed that they would lose their invasive, mesenchymal characteristics, and would instead become more epithelial-like and contribute to tumor outgrowth.

To investigate this hypothesis, we first established that the Ca1h cells have the same marker profile as mesenchymal stem cells and explored the expression of these markers on epithelial-like cells using flow cytometry and immunofluorescent staining. Interestingly, we found that the Ca1a cells and the Ca1hFN30 cells which both have an epithelial-like phenotype have decreased expression of these markers. Using lentiviral transduction, a CD90 knockdown in the mesenchymal-like Ca1h cells was created and characterized. We specifically examined their expression of E-cadherin and fibronectin, an epithelial and mesenchymal marker respectively. Lastly, we evaluated the microenvironmental influence on the CD90 knockdowns using a fibronectin-coated scaffold system and 3D cocultures. Overall, these studies suggest that CD90 is necessary to retain a mesenchymal phenotype and future therapies developed against CD90 may impede metastasis.

2. METHODS

2.1 Culturing Methods

Ca1a and Ca1h cell lines were provided by Dr. Fred Miller (Wayne State University, Detroit, MI). Adipose derived mesenchymal stem cells, ASCs, were purchased from Zenbio. Depletion of fibronectin in the Ca1h cell line was achieved through lentiviral transduction of TRCN0000064830, and selected using puromycin [12]. These cell lines were cultured in DMEM/High Glucose media with 10% fetal bovine serum and 1% penicillin- streptomycin at 37°C in 5% CO₂. Lentiviral transduction was used to stably express dtomato (Ca1a) to allow for cell tracking in coculture through fluorescence.

K562 cells, used as a negative control for flow cytometry studies, were purchased from ATCC and cultured in RPMI media with 10% fetal bovine serum and 1% penicillin- streptomycin at 37°C in 5% CO₂.

2.2 Generation of Ca1h CD90 Knockdown Cell Line

Ca1h cells were used and cultured in the media stated above. Depletion of CD90/THY-1 was achieved through lentiviral-mediated transduction of shRNA V3SVHSHC_5684606 (TH02), V3SVHSHC_7646522 (TH03) (Horizon Discovery/Dharmacon) or a nontargeting scrambled control shRNA. Expression was selected for using puromycin. Further sorting of the depleted population was done using MACS sorting (Miltenyi Biotec, QuadroMACS Separator) with the LD columns (Miltenyi Biotec, Cat:130-042-901) and CD90 MicroBeads (Miltenyi Biotec, Cat: 130-096-253). Cells were labeled with the CD90 magnetic microbeads and passed through the LD columns. Cells that were CD90⁺ magnetically adhered to the column, while those that were CD90⁻ were passed through the column and were collected. Knockdown efficiency and MACS sorting effectiveness was confirmed using flow cytometry.

2.3 Flow Cytometry

Cells were stained at a concentration of 100,000 cells per 100 ul of 3% FBS in PBS. Two panels were created, with staining volumes determined through titration. In panel one, cells were stained with 2 ul of CD90 APC (BD, Cat: 559869), CD105 PE (BD, Cat: 560839), and CD73 PeCy7 (BD,

Cat: 561258). In panel two, cells were stained with 5 ul CD24 PeCy7 (Biolegend, Cat: 311120) and 2 ul CD44 APC (BD, Cat: 559942). Zombie violet (ThermoFisher) was used as a live dead stain with 1 ul per 1×10^6 cells. Isotype controls were used for all conditions. Cells were fixed in 2% PFA in 3% FBS in PBS. The surface marker expression was analyzed using flow cytometry (BD Fortessa) with an average of 10,000 events collected for each group.

2.4 Immunofluorescence

Cells were seeded on chamber slides (Lab-Tek 4 well Chamber Slide) with 1.1×10^4 cells/cm² and cultured until confluence. Once confluent, cells were fixed in 4% paraformaldehyde for 30 minutes, permeabilized in 0.1% triton-X 100 for 5 minutes and blocked with 1% BSA in PBS for 30 minutes. The cells were then labeled with fibronectin (primary antibody: secondary antibody: Invitrogen, Ref: A11008) or phalloidin (ThermoFisher, Cat: A12380) and Ecadherin (primary antibody: BD, Cat: 610182, secondary antibody: Invitrogen, Ref: A11001). The nucleus of the cells were then stained with Hoescht. Fluorescence intensity analysis was performed on immunofluorescent images staining for fibronectin using ImageJ. The mean intensity over all pixels in the green channel was taken.

2.5 Evaluation of Fibronectin Production

To produce the conditioned media, cells were seeded at a density of 1×10^3 cells/cm² in a 6-well plate (Corning Cell Culture plate). After 24 hours, the cells were cultured in serum free media (DMEM/High Glucose) with 1% penicillin/streptomycin. After 36 hours, the media was collected, passed through a 0.2um filter, and stored at -80°C. After the media was collected, the cells were washed with PBS, detached using trypsin, and counted. The cells were spun down at 180g for 5 minutes at 24°C, and the pellet was resuspended in Pierce RIPA buffer (Thermoscientific) at a concentration of 5×10^6 cells/mL. The suspensions were then placed on a shaker in ice for 30 minutes. The lysed samples were then store at -20°C until they were analyzed.

To assess the amount of fibronectin produced, an ELISA assay was performed (Human ELISA Fibronectin kit; Abcam). An aliquot of conditioned media was thawed and evaluated for each cell type. A cell lysate sample for each cell type was also thawed and spun down at 14,000g for 10 minutes before use. Each sample was evaluated along with the appropriate standard curve

following the protocol provided by the manufacturer. Endpoint reading was taken using a Cytation 5 spectrophotometer (Biotek). Analysis of the standard curve and data was done by fitting a 4-parameter logistic regression using Prism.

2.6 Fibronectin Coated Scaffold System

Scaffolds were produced and coated as described by Shinde et al [12]. Cells were seeded onto fibronectin coated scaffolds at a density of 200,000 cells per scaffold. They were cultured for two days and then removed using trypsin. Cells were then stained with CD24, CD44 and CD90 according to the protocol above.

2.7 Cell Proliferation 3D Coculture Assay

Fluorescently labeled Ca1a cells were used to track growth and migration within collagen hydrogels. The collagen gels were created by mixing 8 mg/ml rat tail type I collagen (Corning), with 10X PBS, sodium hydroxide, and a concentrated cell solution consisting of 3×10^6 cells in 100ul of DMEM. The final concentration of collagen was 2.0 mg/ml with a pH of 7.4 and a final cell concentration of 3×10^6 cells/ml. This mixture was then loaded into iBidi u-slide chemotaxis chambers according to the protocol provided by the manufacturer. To polymerize the collagen, loaded slides were placed in an incubator at 37°C for 30 minutes. 5% FBS in DMEM was loaded into both sides after polymerization. Cells were imaged on a Leica DMI6000 for 5 days, imaging every hour and a half.

A generalized multi-parametric particle tracking algorithm was used to quantify the number of Ca1a cells per image frame and the trajectory of individual cells across a time series. Detailed steps of the cell segmentation, including fluorescent image-preprocessing, cell identification, boundary segmentation, parameterization, and tracking can be found in the referenced literature [13], [39]–[42].

2.8 Statistical Analysis

Statistical analysis was performed with Prism software. A one-way ANOVA was used to determine statistical significance between groups. A Tukey test was used to determine significant

differences between means with a p-value of 0.05. Statistical significance is denoted in figures with an asterisk ($p < 0.05$).

3. RESULTS

3.1 Expression of MSC markers in epithelial and mesenchymal-like cells

We used flow cytometry to identify whether the classic mesenchymal stem cell markers, CD90, CD105, and CD73 were present on the MCF10CA1a (Ca1a), MCF10CA1h (Ca1h), and fibronectin knockdown Ca1hFN30. Adipose derived mesenchymal stem cells (ASC) were used as a positive control, and K562 cells, a myeloid leukemia cell line, as the negative control (Figure 3). The gating for each marker was based off the ASCs. On average, $98.90\% \pm 0.45$ of the ASCs were CD90⁺, $97.8\% \pm 0.6$ were CD105⁺, and $99\% \pm 0.26$ were CD73⁺.

The Ca1h cells were positive for all three markers, with a mean of $99.5\% \pm 0.32$ for CD90⁺, $90\% \pm 0.45$ for CD105⁺, and $93.6\% \pm 10.48$ for CD73⁺ (Figure 4). There was no significant difference between the percentage of populations displaying each of the markers on Ca1h and ASCs. However, there was a significant difference between the Ca1a cells and the Ca1h cells. These cells on average had a population of $0.76\% \pm 0.51$ for CD90⁺, and $0.37\% \pm 0.25$ for CD105⁺, while the CD73⁺ population was on average $4.86\% \pm 3.78$. The Ca1h fibronectin knockdowns (Ca1hFN30) also showed a significant decrease in the positive population for each of the markers compared to the Ca1h cells. These cells had a mean population of $2.14\% \pm 3.12$ of CD90⁺ cells, $1.66\% \pm 1.15$ of CD105⁺ cells, and $23.28\% \pm 18.38$ of CD73⁺ cells.

Immunofluorescence staining was used to verify the results from flow cytometry (Figure 5). CD90 and CD105 are present in the ASC and Ca1h cells but are not found in the Ca1a and Ca1hFN30 cells. Interestingly, CD73 was observed in all cell types, appearing much brighter than expected.

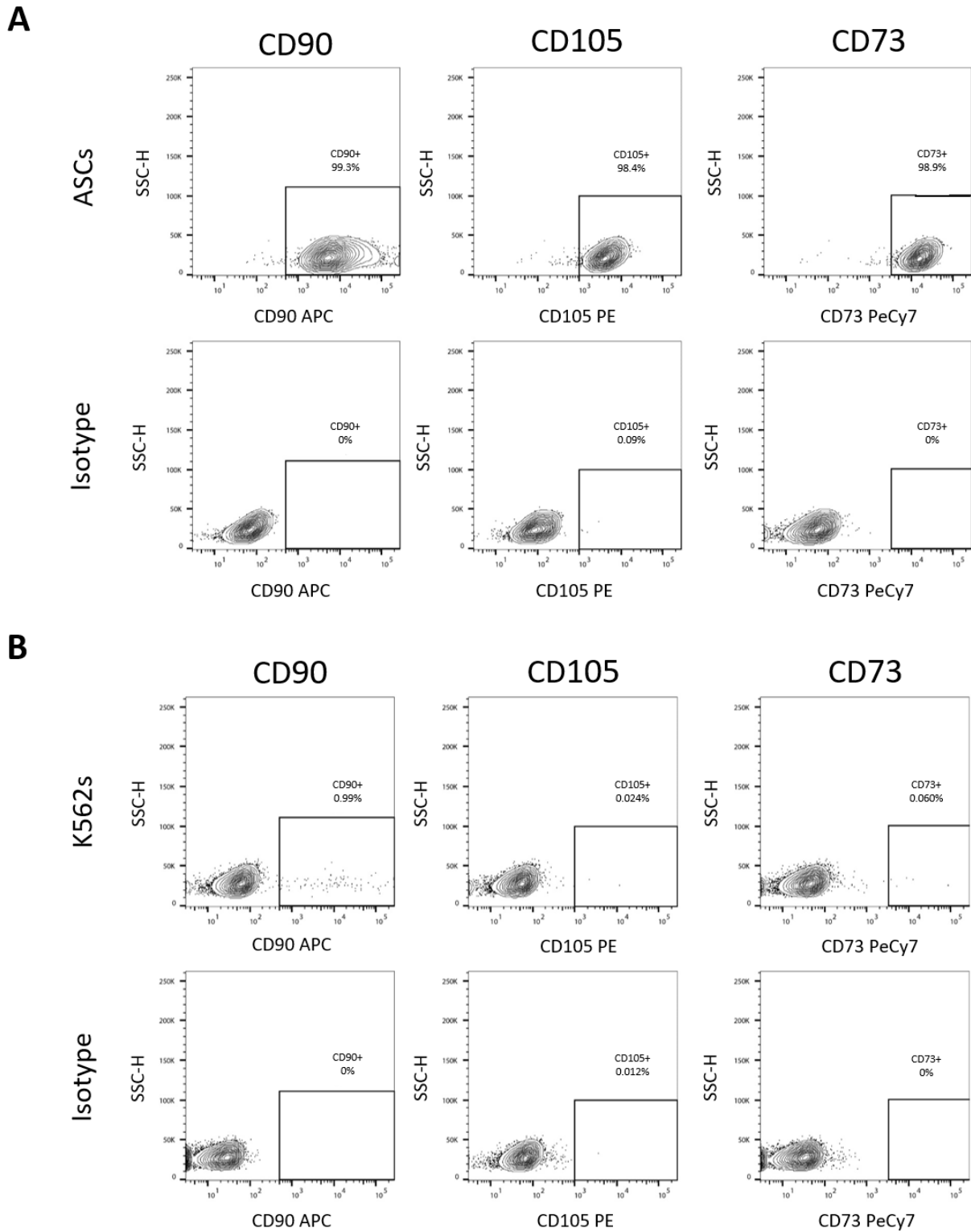


Figure 3. Positive and negative controls for MSC marker analysis. A.) ASCs as a positive control and their isotype stained for CD90, CD105, and CD73. B.) K562s as a negative control and their isotype stained for CD90, CD105, and CD73.

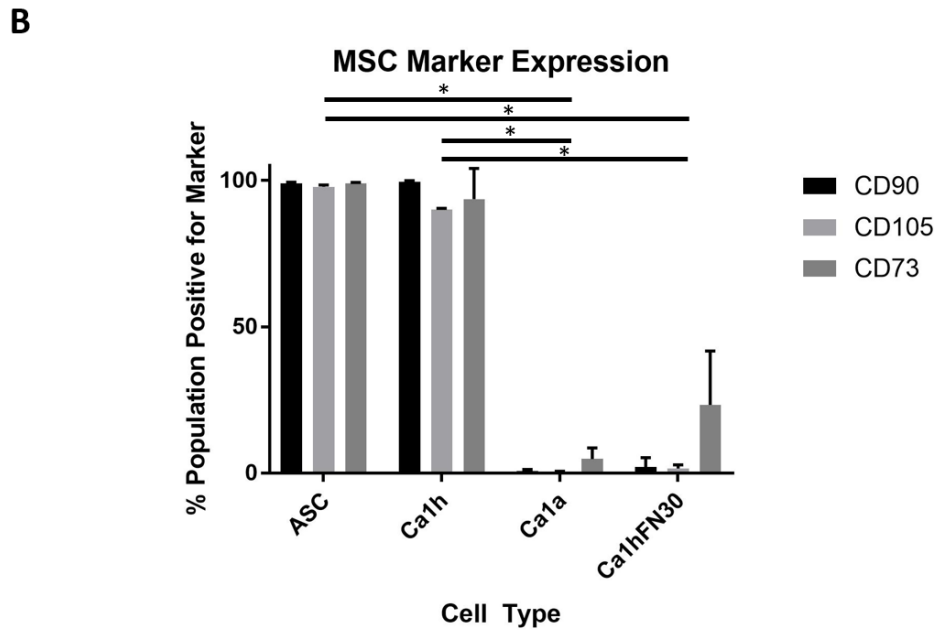
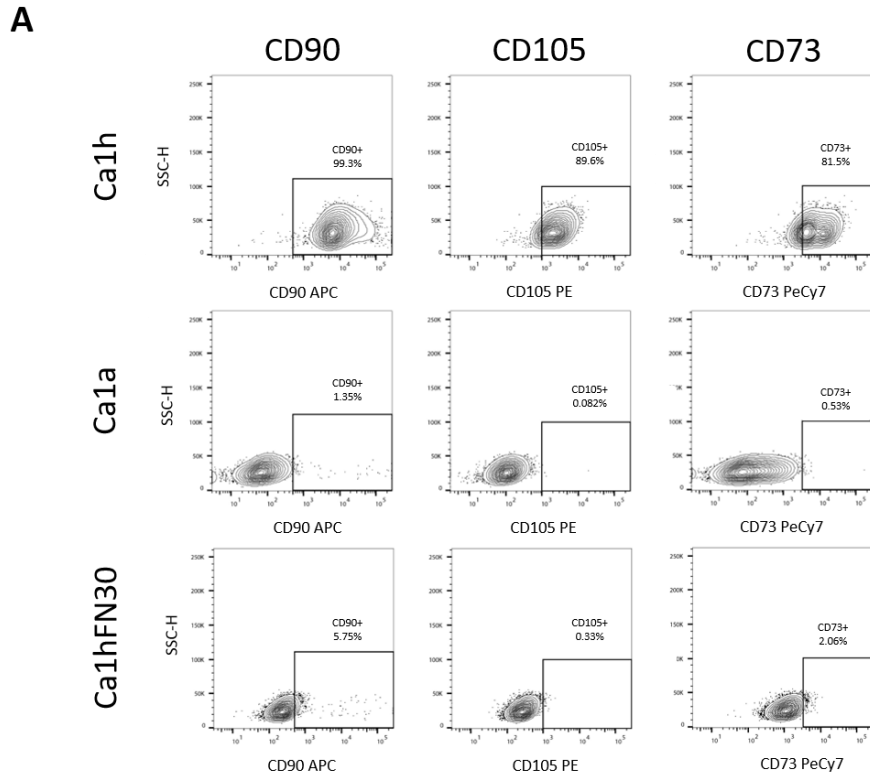


Figure 4. Mesenchymal-like cells express MSC markers, while epithelial-like cells do not.

A.) Flow cytometry graphs showing gating of markers. **B.)** Percent expression of markers in ASC, Ca1h, Ca1a, Ca1hFN30 (n=3). An ANOVA followed by a Tukey test was performed for statistical analysis. Asterisk denotes statistically significant differences in the populations ($p < 0.05$).

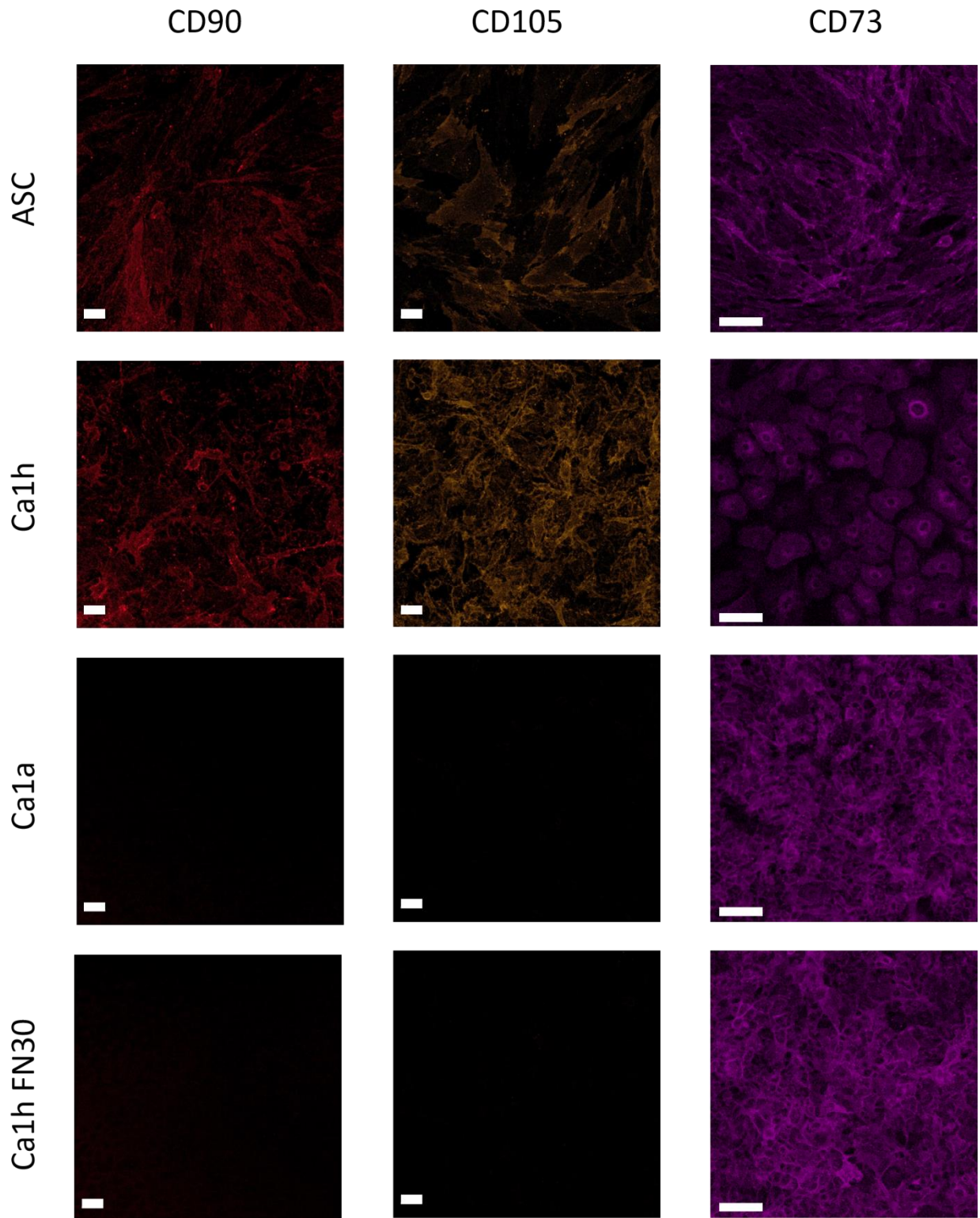


Figure 5. Immunofluorescence images of MSC markers confirm flow cytometry analysis. CD90 in red, CD105 in yellow, CD73 in magenta on ASC, Ca1h, Ca1a, and Ca1hFN30. All scale bars indicate 50 μ m.

3.2 Characterization of CD90 Knockdowns

A CD90 knockdown in the Ca1h cells was created using lenti-viral transduction. Two different shRNA were used, TH02 and TH03, as well as a scramble control. The population of CD90⁺ cells was assessed using flow cytometry (Figure 6A, 6B). The TH03 cells showed more efficiency in knockdown, with an average population of 8.17%±1.45 CD90⁺ cells. The TH02 cells had a lower knockdown efficiency with an average population of 17.67% ± 9.29 expressing CD90. There was no significant difference in CD90⁺ populations for each knockdown. However, a statistically significant difference was seen between the scram CD90⁺ population and the knockdowns. The Ca1h scram continued to express a mean of 97.46%± 1.41. The TH03 cells were used for future studies as they showed a greater reduction and less variability in the CD90⁺ population of cells.

Phenotypic changes were observed in the CD90 knockdowns (Figure 7). In the TH03 cells, which has a lower average population of CD90⁺ cells relative to the TH02 cells, the overall shape of the cells had shifted to more of an epithelial-like phenotype. The TH02 cells, which had a slightly larger CD90⁺ population of cells relative to the TH03 cells, appeared to have a more mesenchymal-like phenotype. They appear unorganized and lack the tight cell-cell junctions seen in epithelial cells [34]. The expression of the EMT marker E-cadherin (E-cad) was also evaluated in each knockdown cell line (Figure 8). This protein is present in more epithelial-like cells as it maintains tight junctions [10]. E-cad expression was seen in both knockdowns. In the TH02 cells, E-cad expression was brighter, but not junctional and more punctate, found mainly around the nucleus of the cell. In the TH03 cells, the expression was lightly distributed throughout the cells.

The CD90 knockdowns were also evaluated for the presence of the CD44/CD24 population of cells (Figure 6C, 6D). It has been shown that breast cancers with CD44⁺/CD24^{-/low} have increased invasion and metastasis, making these a marker for EMT [43]. Though 97.5%±1 Ca1h scram cells were found to be CD44⁺/CD24⁻, the knockdowns had a significantly lower population of CD44⁺/CD24⁻. The TH02 cells had an average of 61.1%±17.4 of cells that are CD44⁺/CD24⁻, while the TH03 cells had 68.8%±5.9. There was no statistical difference between the TH02 and TH03 CD44⁺/CD24⁻ populations.

This E-cad expression change in the CD44⁺/CD24⁻ population distribution, and the change in phenotype suggests that CD90 may be necessary to maintain a mesenchymal phenotype.

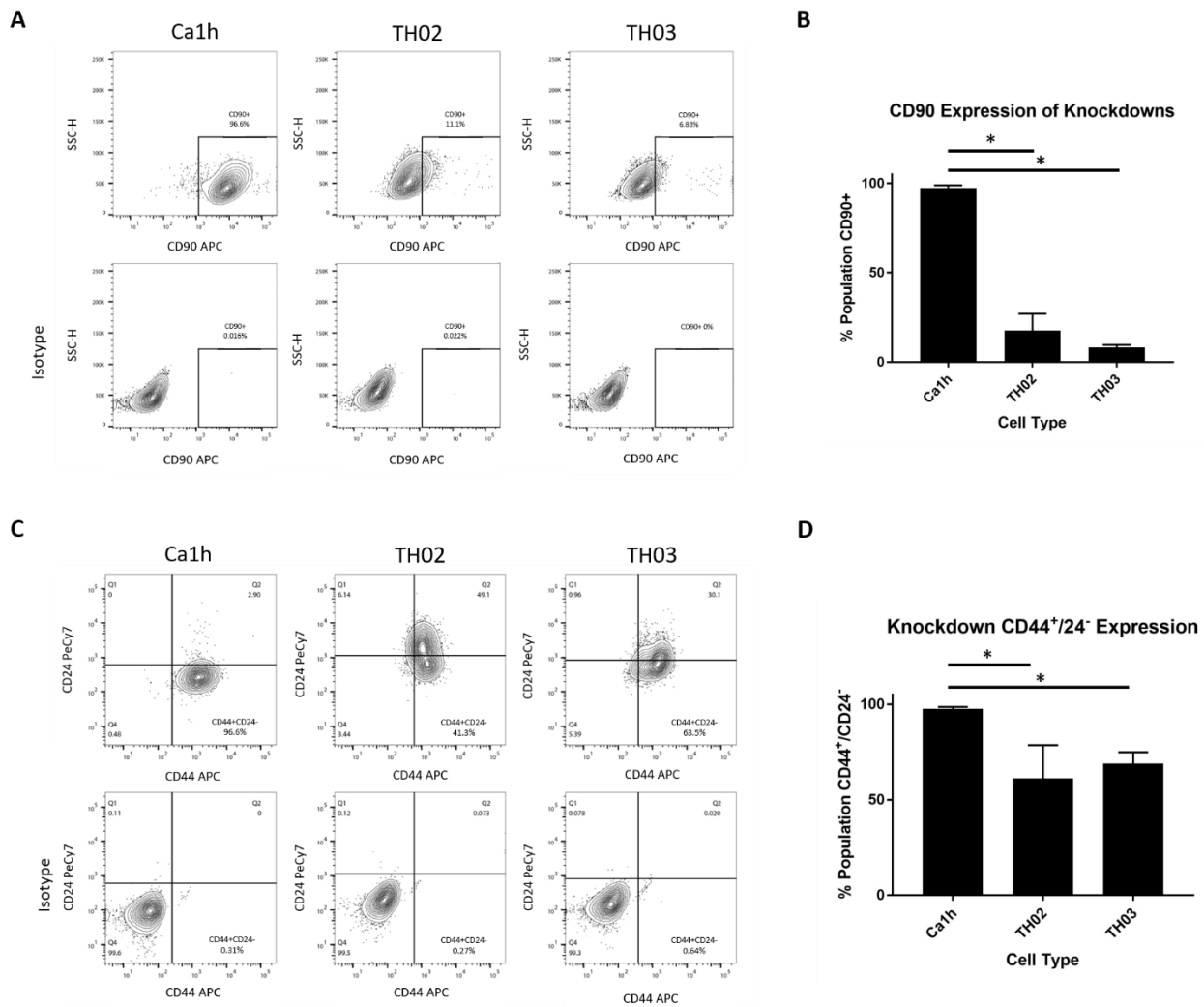


Figure 6. Characterization of CD90 knockdowns using flow cytometry. A.) Flow cytometry graphs showing gating of CD90. **B.)** Percent expression of CD90 in wild type Ca1h, and knockdowns TH02 and TH03 (n=3). **C.)** Flow cytometry graphs showing gating of CD24 and CD44. **D.)** Percent expression of CD44⁺/CD24⁻ in wild type Ca1h, and knockdowns TH02 and TH03 (n=3). An ANOVA followed by a Tukey test was performed for statistical analysis. Asterisk denotes statistically significant differences in the populations ($p < 0.05$).

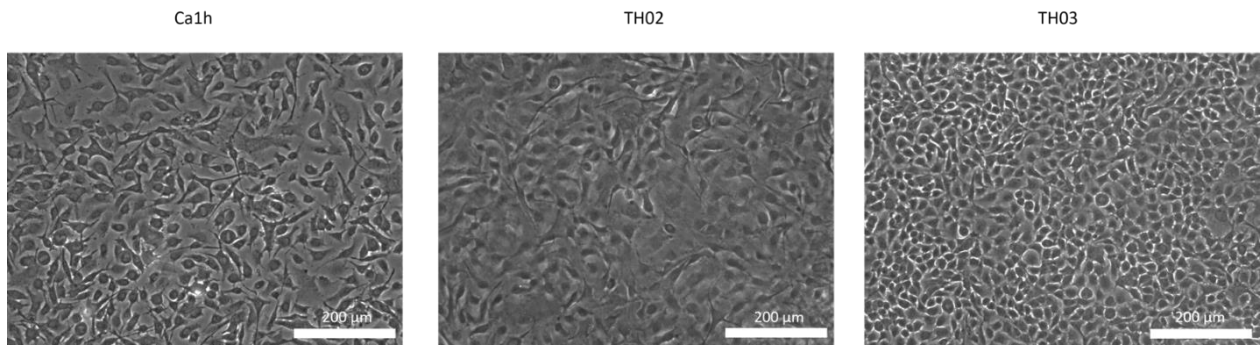


Figure 7. CD90 knockdown shows transition to epithelial-like phenotype. Phase contrast images of scram Ca1h and CD90 knockdowns.

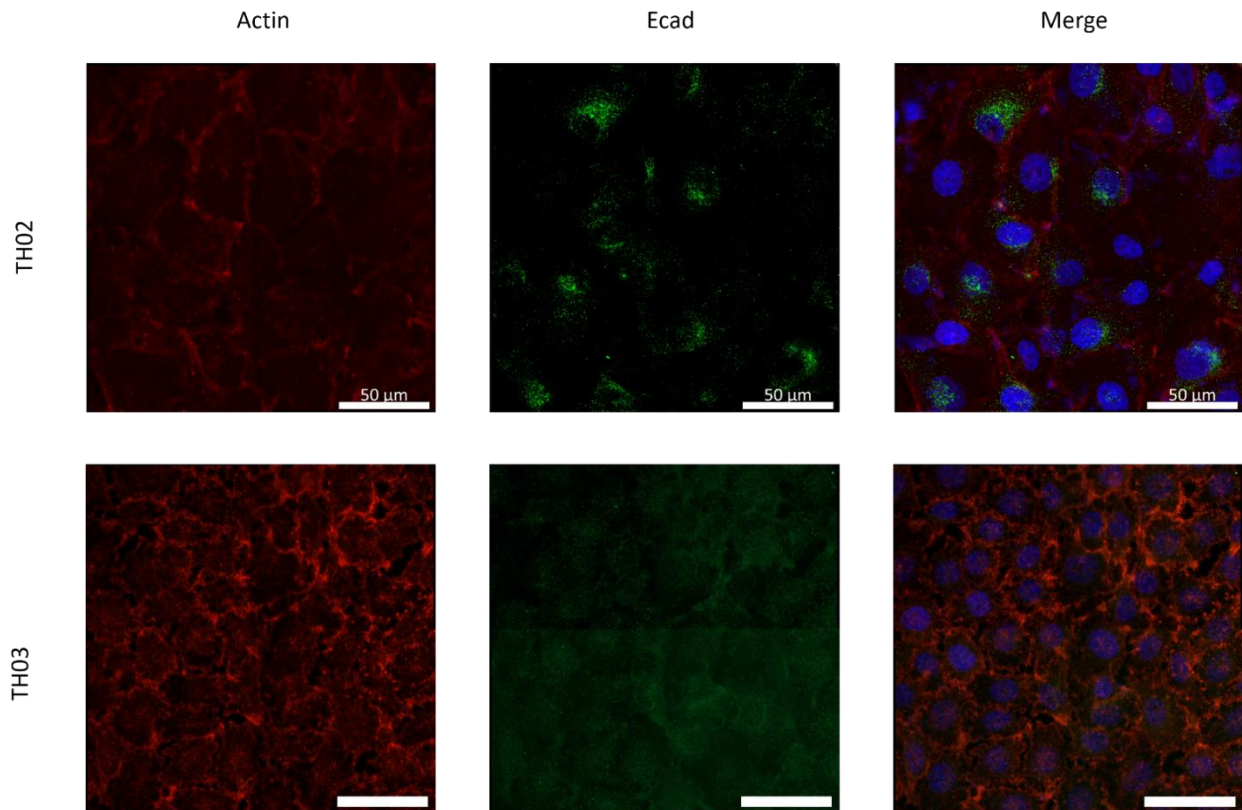
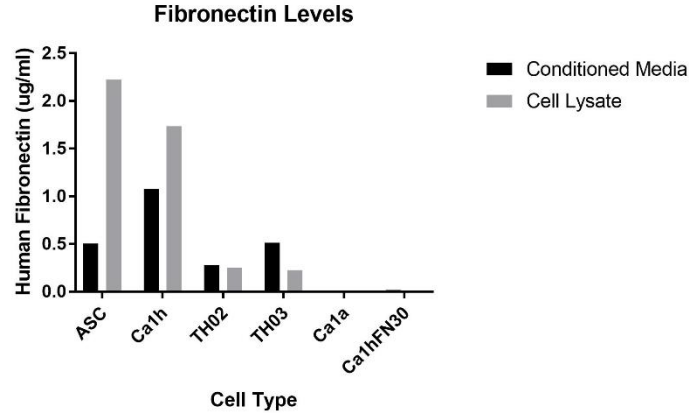


Figure 8. CD90 knockdowns shows expression of E-cadherin.

3.3 Fibronectin Expression

Using an ELISA, it was found that cells that are CD90 positive produce more fibronectin, a mesenchymal marker, in both the conditioned media and whole cell lysate (Figure 8A). The Ca1a cells contained 0.004 $\mu\text{g/ml}$ fibronectin in the conditioned media, and 0.002 $\mu\text{g/ml}$ in cell lysate. Similarly, the Ca1hFn30 showed low levels of fibronectin with 0.019 $\mu\text{g/ml}$ in conditioned media, and 0.01 $\mu\text{g/ml}$ in cell lysate. As expected, elevated levels of fibronectin were found in both the conditioned media and cell lysate of the Ca1h cells with 1.076 $\mu\text{g/ml}$ in conditioned media, and 1.736 $\mu\text{g/ml}$ in cell lysate. The ASCs also produced high levels of fibronectin with 0.508 $\mu\text{g/ml}$ found in conditioned media and 2.224 $\mu\text{g/ml}$ in cell lysate. By knocking down CD90 in the Ca1h cells, fibronectin expression in both the conditioned media and cell lysate decreased. The TH02 cells had 0.281 $\mu\text{g/ml}$ in conditioned media and 0.250 $\mu\text{g/ml}$ in cell lysate, while the TH03 cells had 0.514 $\mu\text{g/ml}$ in conditioned media, and 0.228 $\mu\text{g/ml}$ in cell lysate. Confocal microscopy confirmed the presence of fibronectin, the most of which was present in the ASCs (Figure 8B). The fluorescence intensity analysis of these images using ImageJ showed that the ASCs had a mean fluorescence of 34.6, and the Ca1a cells had a mean fluorescence of 0.46. The Ca1h cells had a mean of 7.33 while the TH02 had a mean of 8.13. The TH03 had a lower fluorescence intensity with an average of 1.825. Though the ELISA showed that the knockdown cell lines express less fibronectin than the Ca1h cells, this was not seen in the image analysis.

A



B

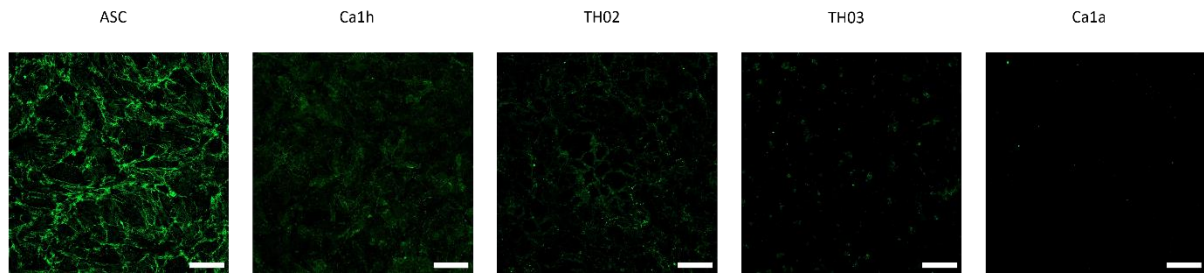


Figure 9. CD90 knockdowns still express fibronectin. A.) Human fibronectin ELISA results in ug/ml. B.) Immunofluorescence staining for fibronectin. Fluorescence intensity analysis was done using ImageJ. Scale bar indicates 100 μ m.

3.4 Early Metastatic Niche Model

Cells were cultured on a fibronectin coated scaffold to better understand how the metastatic niche may alter the cancer cell phenotype. Previous studies have shown that the CD90⁺ population of AT-3 cells and the CD44⁺/CD24⁻ population of MDA-MB-468 cells increases when cells are cultured a fibronectin rich environment [33]. After culturing cells for two days on fibronectin coated scaffolds, we demonstrated an increase in the CD44⁺/CD24⁻ for the TH03, and Ca1a cells (Figure 10). The Ca1a cells saw an increase CD44⁺/CD24⁻ population from 20.7% to 85.5%. The TH03 cells also saw an increase from 63.5% to 90.4%. The Ca1h cells maintained their CD44⁺/CD24⁻ population at 96% on scaffolds. A shift in CD90⁺ population was not observed (Figure 11). The Ca1h cells retained their CD90⁺ population with 97.9% CD90⁺ cells. The TH03 knockdowns had a population of 3.14% of CD90⁺ which was lower than the established baseline. The Ca1a CD90⁺ population was 0.11%.

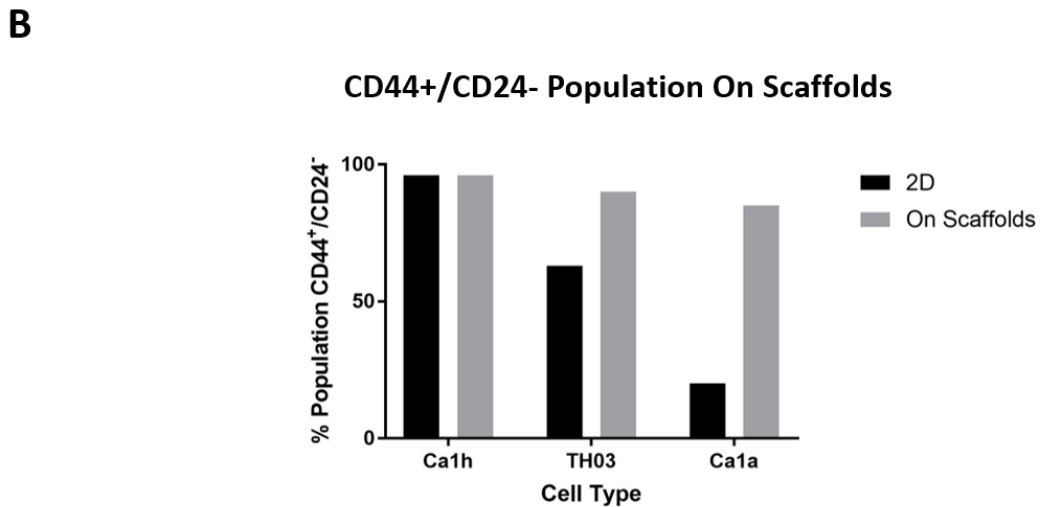
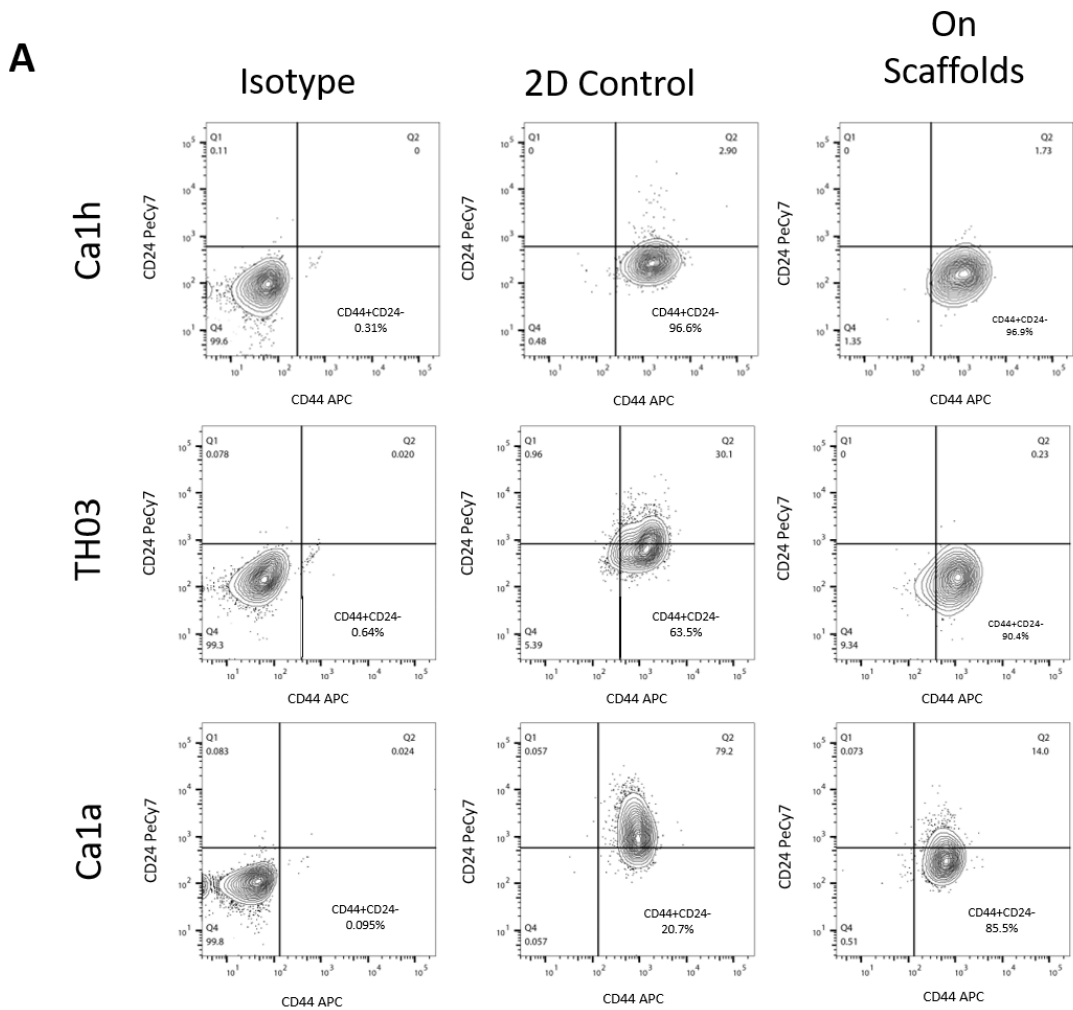


Figure 10. CD44⁺/CD24⁻ populations increased after culturing on fibronectin coated scaffolds. A.) Flow cytometry graphs showing gating of CD44⁺/CD24⁻ population. **B.)** Percent of population that is CD44⁺/CD24⁻ on scaffolds in comparison to 2D (n=1).

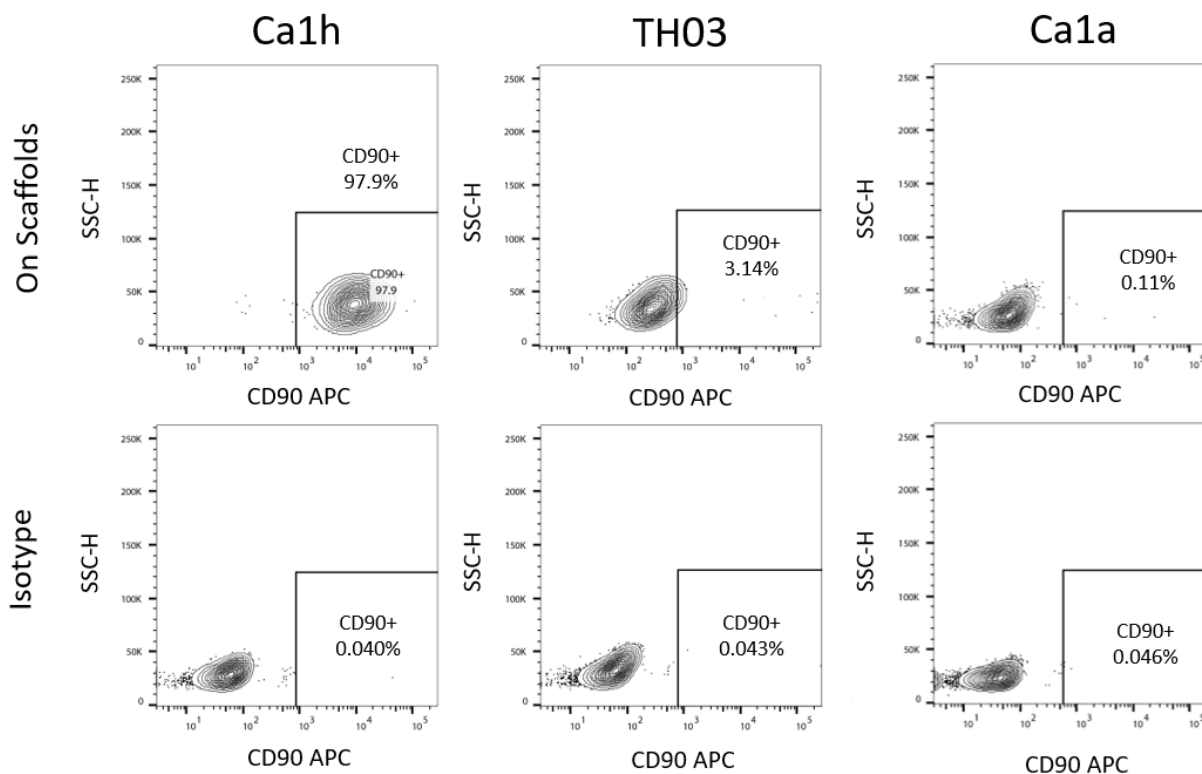


Figure 11. CD90⁺ population does not shift after culturing on fibronectin coated scaffolds. Flow cytometry analysis for Ca1h, TH03, and Ca1a cultured on scaffolds (n=1).

3.5 Effect of Coculture on Cell Proliferation

To assess the effect of CD90 on cell survival, we performed a cell proliferation assay by placing Ca1a cells alone or in a coculture in a collagen gel (Figure 12). The coculture of the ASCs and Ca1as showed the most growth over 3 days, with a normalized final cell count of 3.6 ± 0.86 fold of the initial seeding. The Ca1a growth was limited when cultured with TH03 cells, with a final normalized count of 1.7 ± 0.21 fold of the initial seeding, while the monoculture of Ca1a had a normalized cell count of 2.25 ± 0.33 fold of the initial seeding. A significant difference between the proliferation of the Ca1a cells in coculture with the ASCs and of the Ca1a cells in coculture with the TH03 (Figure 12B) was observed.

The distance traveled by the Ca1a cells was also calculated. The Euclidean distance was similar between all conditions, with no statistical differences observed. Alone, the Ca1a average Euclidean distance was $7.81 \pm 0.07 \mu\text{m}$, while in a coculture with ASC the mean was $9.02 \pm 0.16 \mu\text{m}$, and in coculture with the TH03 the mean Euclidean distance was $8.13 \pm 0.24 \mu\text{m}$. When cultured

alone, the accumulated distance the Ca1a cells was $22.75 \pm 2.22 \mu\text{m}$. This was significantly greater than the migration of Ca1a cells in a coculture with ASCs. The accumulated distance traveled for the Ca1a cells was $16.5 \pm 0.74 \mu\text{m}$. There was also a significant difference in migration between the Ca1a cells with the ASCs and the Ca1a cells with the TH03 cells. With the TH03 cells, the accumulated distance was $26.63 \pm 1.03 \mu\text{m}$.

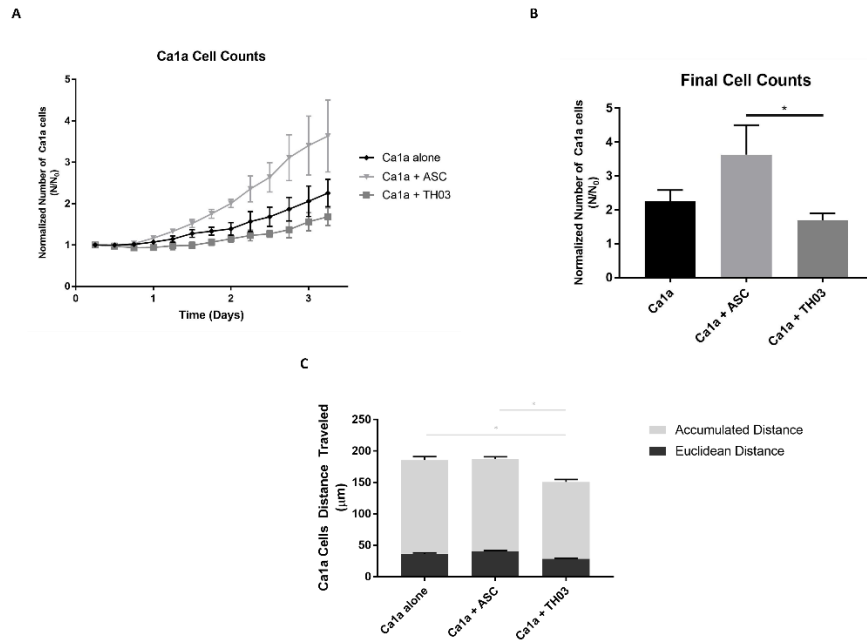


Figure 12. Coculture analysis shows increase proliferation and migration of Ca1a when cocultured with ASCs compared to TH03. A.) Normalized proliferation of Ca1a cells alone and in coculture over 3.25 days. **B.)** Final normalized cell count on day 3.25 of coculture. **C.)** Distanced traveled by Ca1a cells in μm . An ANOVA followed by a Tukey test was performed for statistical analysis. Asterisk denotes statistically significant differences in the populations ($p < 0.05$).

4. DISCUSSION

Previously, we have demonstrated that heterogenous mosaic tumors have different metastatic potential than a homogenous tumor. Ca1h cells have been shown to enhance metastasis of the Ca1a epithelial cells in vivo, however Ca1a cells alone do not have the ability to metastasize [12]. We believe that the Ca1h cells behave like mesenchymal stem cells, which have been shown to promote tumor outgrowth in breast cancer [34]. We evaluated the Ca1h cells for the classic MSC markers CD90, CD105, and CD73. We found that these same stem markers are present on Ca1h mesenchymal-like cells and are not expressed on the Ca1a epithelial-like cells. Interestingly, fibronectin expression also alters the expression levels of these markers. By knocking down fibronectin, the expression of CD90 and CD105 in the mesenchymal-like cells is lost, with some change to CD73 expression. This suggests that fibronectin may be a key protein in maintaining a stem cell niche.

Patient data presented suggests that expression of CD90 influences patient survival. CD90 is expressed on the invasive front of tumors and surrounding the tumor itself, indicating more mesenchymal-like properties [37], [38]. Genetic depletion of CD90 in mesenchymal-like cells led to a more epithelial-like cell line. CD90 has been shown to regulate cellular adhesion, cytoskeletal organization, and can create distinct morphologies in fibroblasts [44], [45]. Similarly, in the CD90 knockdowns we noticed a change in morphology where they seemed to be more tightly packed with a less spread out phenotype. These cells also showed a reduction in fibronectin production and showed signs of changing phenotype, while expressing low levels of E-cadherin. However, more studies should be done to confirm this transition to an epithelial-like state.

Previous studies have shown that Ca1a cells rely on Ca1h cells in vivo and in vitro [12], [13]. Ca1h cells assist the Ca1a cells and cause increased migration and proliferation of these cells in a coculture [13]. Here, we demonstrate the ASC cells behave similarly, furthering the idea that Ca1h cells play a role in the tumor microenvironment comparable to that of MSCs. We also show that knocking down CD90 results in a loss of this supportive capability, reducing proliferation and migration of the Ca1a cells. These findings suggest that CD90 may play an important role in tumor outgrowth.

Breast cancer stem cell marker expression was also assessed after culturing on fibronectin coated scaffolds. CD44⁺/CD24⁻ populations have been identified as a tumor initiating population,

and have increased metastatic properties [46], [47]. All cell types, Ca1a, Ca1h, and CD90 knockdown showed an increase in CD44⁺/CD24⁻ population suggesting that fibronectin rich environments increase tumorigenicity. However, a shift in the CD90⁺ population is not seen while culturing in this environment, unlike what was observed in previous studies [33].

Here we show that CD90 may play an important role in tumor progression, however more studies need to be completed. First, an animal study using a murine model will be performed with the CD90 knockdowns to assess the effects *in vivo*. Though the TH03 cells have begun to look and behave like epithelial cells, a complete knockout of the THY1 gene should confirm these results. It would also be interesting to assess the influence of a CD90 knock in on the epithelial like Ca1a to evaluate whether the changes we are seeing can be reversed.

In conclusion, we believe CD90 plays an important role in breast cancer tumor progression by perpetuating a mesenchymal-like phenotype, allowing cells to take a supportive role in the tumor microenvironment. The change in morphology, increase expression of epithelial markers, and the decrease in fibronectin expression show a switch to an epithelial phenotype. The CD90 knockdown behavior in coculture with the epithelial cells also supports this, as they reduce proliferation and migration. These findings suggest that CD90 could be a potential target for therapies to prevent the metastasis of breast cancer.

REFERENCES

- [1] R. L. Siegel, K. D. Miller, and A. Jemal, “Cancer statistics, 2020,” *CA. Cancer J. Clin.*, vol. 70, no. 1, pp. 7–30, Jan. 2020.
- [2] C. E. DeSantis *et al.*, “Breast cancer statistics, 2019,” *CA. Cancer J. Clin.*, vol. 69, no. 6, pp. 438–451, Nov. 2019.
- [3] A. W. Lambert, D. R. Pattabiraman, and R. A. Weinberg, “Emerging Biological Principles of Metastasis,” *Cell*, vol. 168, no. 4. Cell Press, pp. 670–691, 09-Feb-2017.
- [4] J. A. Joyce and J. W. Pollard, “Microenvironmental regulation of metastasis,” *Nature Reviews Cancer*, vol. 9, no. 4. Nature Publishing Group, pp. 239–252, 12-Apr-2009.
- [5] D. Hong *et al.*, “EMT and Cancer Stem Cells contribute to Breast Cancer Heterogeneity,” vol. 233, no. 12, pp. 9136–9144, 2019.
- [6] J. M. Rosen and K. Roarty, “Paracrine signaling in mammary gland development: What can we learn about intratumoral heterogeneity?,” *Breast Cancer Research*, vol. 16, no. 1. BioMed Central, p. 202, 19-Jan-2014.
- [7] A. Shinde, J. S. Paez, S. Libring, K. Hopkins, L. Solorio, and M. K. Wendt, “Transglutaminase-2 facilitates extracellular vesicle-mediated establishment of the metastatic niche,” *Oncogenesis*, vol. 9, no. 2, pp. 1–12, Feb. 2020.
- [8] O. J. Scully, B.-H. Bay, G. Yip, and Y. Yu, “Breast cancer metastasis.,” *Cancer Genomics Proteomics*, vol. 9, no. 5, pp. 311–20, Sep. 2012.
- [9] Y. Zhang and R. A. Weinberg, “Epithelial-to-mesenchymal transition in cancer: complexity and opportunities EMT: a naturally occurring transdifferentiation program Basics of the EMT program Compliance with ethics guidelines HHS Public Access,” *Front Med*, vol. 12, no. 4, pp. 361–373, 2018.
- [10] W. Lu and Y. Kang, “Epithelial-Mesenchymal Plasticity in Cancer Progression and Metastasis,” *Developmental Cell*, vol. 49, no. 3. Cell Press, pp. 361–374, 06-May-2019.
- [11] S. S. Sikandar *et al.*, “Role of epithelial to mesenchymal transition associated genes in mammary gland regeneration and breast tumorigenesis,” *Nat. Commun.*, vol. 8, no. 1, Dec. 2017.
- [12] A. Shinde *et al.*, “Autocrine fibronectin inhibits breast cancer metastasis,” *Mol. Cancer Res.*, vol. 16, no. 10, pp. 1579–1589, Oct. 2018.

- [13] L. Jun, B., Guo, T., Libring, S., Chanda, M., Paez, J.S., Shinde, A., Wendt, M., Vlachos, P., & Solorio, “Fibronectin-expressing Mesenchymal Tumor Cells promote Breast Cancer Metastasis,” 2020.
- [14] G. Barriere, P. Fici, G. Gallerani, F. Fabbri, and M. Rigaud, “Epithelial Mesenchymal Transition: a double-edged sword,” *Clin. Transl. Med.*, vol. 4, no. 1, pp. 1–6, Dec. 2015.
- [15] R. C. Stone *et al.*, “Epithelial-mesenchymal transition in tissue repair and fibrosis,” *Cell and Tissue Research*, vol. 365, no. 3. Springer Verlag, pp. 495–506, 01-Sep-2016.
- [16] M. S. Hu, M. R. Borrelli, H. P. Lorenz, M. T. Longaker, and D. C. Wan, “Mesenchymal Stromal Cells and Cutaneous Wound Healing: A Comprehensive Review of the Background, Role, and Therapeutic Potential,” *Stem Cells Int.*, vol. 2018, 2018.
- [17] B. G. Cuiffo and A. E. Karnoub, “Mesenchymal stem cells in tumor development: Emerging roles and concepts,” *Cell Adhesion and Migration*, vol. 6, no. 3. Taylor and Francis Inc., pp. 220–230, 2012.
- [18] R. Ramasamy, E. W. F. Lam, I. Soeiro, V. Tisato, D. Bonnet, and F. Dazzi, “Mesenchymal stem cells inhibit proliferation and apoptosis of tumor cells: Impact on in vivo tumor growth,” *Leukemia*, vol. 21, no. 2, pp. 304–310, Dec. 2007.
- [19] S. M. Albarenque, R. M. Zwacka, and A. Mohr, “Both human and mouse mesenchymal stem cells promote breast cancer metastasis,” *Stem Cell Res.*, vol. 7, no. 2, pp. 163–171, Sep. 2011.
- [20] T. Zhang, W. Y. W. Lee, Y. F. Rui, T. Y. Cheng, X. H. Jiang, and G. Li, “Bone marrow-derived mesenchymal stem cells promote growth and angiogenesis of breast and prostate tumors,” *Stem Cell Res. Ther.*, vol. 4, no. 3, p. 70, Jun. 2013.
- [21] A. E. Karnoub *et al.*, “Mesenchymal stem cells within tumour stroma promote breast cancer metastasis,” *Nature*, vol. 449, no. 7162, pp. 557–563, Oct. 2007.
- [22] B. Ljubic *et al.*, “Human mesenchymal stem cells creating an immunosuppressive environment and promote breast cancer in mice,” *Sci. Rep.*, vol. 3, no. 1, pp. 1–9, Jul. 2013.
- [23] M. Dominici *et al.*, “Minimal criteria for defining multipotent mesenchymal stromal cells. The International Society for Cellular Therapy position statement,” *Cytotherapy*, vol. 8, no. 4, pp. 315–317, Aug. 2006.

- [24] J. A. Ankrum, J. F. Ong, and J. M. Karp, “Mesenchymal stem cells: Immune evasive, not immune privileged,” *Nature Biotechnology*, vol. 32, no. 3. Nature Publishing Group, pp. 252–260, 23-Feb-2014.
- [25] J. Gao *et al.*, “Integrative analysis of complex cancer genomics and clinical profiles using the cBioPortal,” *Sci. Signal.*, vol. 6, no. 269, Apr. 2013.
- [26] E. Cerami *et al.*, “The cBio Cancer Genomics Portal: An open platform for exploring multidimensional cancer genomics data,” *Cancer Discov.*, vol. 2, no. 5, pp. 401–404, May 2012.
- [27] B. Pereira *et al.*, “The somatic mutation profiles of 2,433 breast cancers refines their genomic and transcriptomic landscapes,” *Nat. Commun.*, vol. 7, May 2016.
- [28] K. M. Rau *et al.*, “Neovascularization evaluated by CD105 correlates well with prognostic factors in breast cancers,” *Exp. Ther. Med.*, vol. 4, no. 2, pp. 231–236, Aug. 2012.
- [29] L. C *et al.*, “Plasma Levels of Soluble CD105 Correlate With Metastasis in Patients With Breast Cancer,” *Int. J. cancer*, vol. 89, no. 2, 2000.
- [30] B. Zhang, “CD73: A novel target for cancer immunotherapy,” *Cancer Research*, vol. 70, no. 16. NIH Public Access, pp. 6407–6411, 15-Aug-2010.
- [31] C. Sauzay, K. Voutetakis, A. A. Chatziioannou, E. Chevet, and T. Avril, “CD90/Thy-1, a cancer-associated cell surface signaling molecule,” *Frontiers in Cell and Developmental Biology*, vol. 7, no. APR. Frontiers Media S.A., 2019.
- [32] A. Kumar, A. Bhanja, J. Bhattacharyya, and B. G. Jaganathan, “Multiple roles of CD90 in cancer,” *Tumor Biology*, vol. 37, no. 9. Springer Netherlands, pp. 11611–11622, 01-Sep-2016.
- [33] S. Jordahl *et al.*, “Engineered Fibrillar Fibronectin Networks as Three-Dimensional Tissue Scaffolds,” *Adv. Mater.*, vol. 31, no. 46, p. 1904580, Nov. 2019.
- [34] K. Mandel, Y. Yang, A. Schambach, S. Glage, A. Otte, and R. Hass, “Mesenchymal stem cells directly interact with breast cancer cells and promote tumor cell growth in vitro and in vivo,” *Stem Cells Dev.*, vol. 22, no. 23, pp. 3114–3127, 2013.
- [35] T. H. Barker *et al.*, “Thrombospondin-1-induced focal adhesion disassembly in fibroblasts requires Thy-1 surface expression, lipid raft integrity, and Src activation,” *J. Biol. Chem.*, vol. 279, no. 22, pp. 23510–23516, May 2004.

- [36] A. R. Maia Lobba *et al.*, “High CD90 (THY-1) expression positively correlates with cell transformation and worse prognosis in basal-like breast cancer tumors,” *PLoS One*, vol. 13, no. 6, Jun. 2018.
- [37] V. S. Donnenberg *et al.*, “Localization of CD44 and CD90 positive cells to the invasive front of breast tumors,” *Cytom. Part B - Clin. Cytom.*, vol. 78, no. 5, pp. 287–301, Sep. 2010.
- [38] X. Wang, Y. Liu, K. Zhou, G. Zhang, F. Wang, and J. Ren, “Isolation and characterization of CD105+/CD90+ subpopulation in breast cancer MDA-MB-231 cell line,” *Int. J. Clin. Exp. Pathol.*, vol. 8, no. 5, pp. 5105–5112, 2015.
- [39] N. D. Cardwell, P. P. Vlachos, and K. A. Thole, “A multi-parametric particle-pairing algorithm for particle tracking in single and multiphase flows,” *Meas. Sci. Technol.*, vol. 22, no. 10, p. 105406, Aug. 2011.
- [40] T. Guo, A. M. Ardekani, and P. P. Vlachos, “Microscale, scanning defocusing volumetric particle-tracking velocimetry,” *Exp. Fluids*, vol. 60, no. 6, p. 89, Jun. 2019.
- [41] J. Canny, “A Computational Approach to Edge Detection,” *IEEE Trans. Pattern Anal. Mach. Intell.*, vol. PAMI-8, no. 6, pp. 679–698, 1986.
- [42] P. L. Rosin, “Computing global shape measures,” in *Handbook of Pattern Recognition and Computer Vision, 3rd Edition*, World Scientific Publishing Co., 2005, pp. 177–196.
- [43] W. Li, H. Ma, J. Zhang, L. Zhu, C. Wang, and Y. Yang, “Unraveling the roles of CD44/CD24 and ALDH1 as cancer stem cell markers in tumorigenesis and metastasis,” *Sci. Rep.*, vol. 7, no. 1, pp. 1–15, Dec. 2017.
- [44] T. H. Barker *et al.*, “Thy-1 regulates fibroblast focal adhesions, cytoskeletal organization and migration through modulation of p190 RhoGAP and Rho GTPase activity,” *Exp. Cell Res.*, vol. 295, no. 2, pp. 488–496, May 2004.
- [45] T. A. Rege, M. A. Pallero, C. Gomez, H. E. Grenett, J. E. Murphy-Ullrich, and J. S. Hagood, “Thy-1, via its GPI anchor, modulates Src family kinase and focal adhesion kinase phosphorylation and subcellular localization, and fibroblast migration, in response to thrombospondin-1/hep I,” *Exp. Cell Res.*, vol. 312, no. 19, pp. 3752–3767, Nov. 2006.
- [46] G. B. Jang *et al.*, “Blockade of Wnt/ β -catenin signaling suppresses breast cancer metastasis by inhibiting CSC-like phenotype,” *Sci. Rep.*, vol. 5, no. 1, pp. 1–15, Jul. 2015.

- [47] M. Al-Hajj, M. S. Wicha, A. Benito-Hernandez, S. J. Morrison, and M. F. Clarke, “Prospective identification of tumorigenic breast cancer cells,” *Proc. Natl. Acad. Sci. U. S. A.*, vol. 100, no. 7, pp. 3983–3988, Apr. 2003.